.

Danish Meteorological Institute
Ministry of Transport

Scientific Report 07-02

Idealized simulations of shallow convection using recent HIRLAM physics

Bent H Sass

Contents

1 Dansk resume

Simuleringer af konvektive skyer i atmosfæren under ca. 3 km højde studeres ved hjælp af 1-dimensional søjlemodel af HIRLAM-systemet med fysiske parametriseringer og en specificeret dynamisk forcering. Klassiske experimenter fra internationale studier testes og verificeres bl.a. mod resultater fra 'Large-Eddy' simuleringer. Det vises, at en ny version af HIRLAM-fysik giver væsentligt forbedrede resultater når der sammenlignes med Large-Eddy simuleringer.

2 Abstract

Shallow convection in the atmosphere below a height of about 3 km is studied in 1-dimensional column model simulations using recent HIRLAM physics. Test cases from the litterature such as ASTEX, BOMEX and EUROCS shallow cumulus are performed and checked against corresponding results from Large-Eddy simulations. It is shown that a new version of the physics exhibit considerably better results than a previous version when compared to the results of large eddy simulations.

3 Introduction

The present study is devoted to idealized numerical simulations of shallow convection in the low troposphere. The focus is on the test of turbulence and moist physics parameterizations which are essential for describing these convective phenomena in operational atmospheric models which are typically run with grid sizes between, say 3 and 30 km. At these model resolutions it is not possible to resolve the air motions occurring in the context of shallow convection. The framework for the tests is a column model with physical parameterizations and appropriate specified dynamical forcing for specific convective cases.

More specifically, by shallow convection is meant processes with condensation and latent heat release up to a height of at most 3 km. The horizontal scale of the cloud processes to be parameterized in the 1D-column model may vary considerably depending on the type of case studied. For adequate simulation of the physics the parameterizations will have to describe scales from turbulent eddy size to normal cumulus cloud size. The physical parameterizations studied have been developed for a high resolution limited area model, referred to as HIRLAM. The parameterization of very large mesoscale convective complexes, which can be relevant in coarse mesh models is outside the scope of the present formulation.

It has been shown in various field campaigns over the years that shallow convective clouds in the low troposphere play an important role in transporting heat and moisture upwards in the atmosphere. For example, this was documented already for trade wind non-precipitating clouds during BOMEX, the Barbados Oceanographic and Meteorological EXexperiment (Nitta and Esbensen, 1974).

In recent years it has become possible in atmospheric numerical models to simulate shallow convection, e.g. in the socalled large-eddy simulation models (LES). These models are run at resolutions which make it possible to resolve convective clouds. Thus the BOMEX case has also been studied in LES (Siebesma and Cuipers, 1995). The diagnostic output from the LES has been used for setting up experiments testing the quality of physical parameterizations used in synoptic scale and mesoscale meteorological models of the atmosphere.

In this study the physical parameterizations of HIRLAM, (Undén et al., 2002) are tested for 3 different shallow convective cases which have been described in the litterature (field experiments and the performance of LES).

The first experiment ASTEX, the Atlantic Stratocumulus Transition EXperiment (Bretherton and Pincus, 1995; Albrecht et al., 1995) is concerned with stratocumulus clouds in the Atlantic ocean. The field experiment was specifically designed to study the transition between solid stratocumulus and trade wind cumulus in the subtropics. This case is different from normal shallow cumulus convection because it occurs in very humid conditions where convective instability is generated at the stratiform cloud tops through thermal radiative cooling. The case is well suited for studying the entrainment rate of the cloud layer at the top and the evolution of the internal structure of the cloud layer over time.

The second case is a traditional shallow convection cumulus case, namely the BOMEX case. It was conducted near Barbados in the tropical ocean, and the data set applies to rather stationary conditions with subsidence. The tops of the convective clouds were below 2 km. The observed total fractional cloud amount was rather small (at most 15-20 %) and the clouds were practically non-precipitating.

Finally, the third case, the socalled EUROCS shallow cumulus case, (Brown et al., 2002) is based on LES describing the diurnal variation of shallow cumulus in summer conditions over the Southern Great Planes in the USA. It is constructed from an idealization of observations on 21 June 1997 from the ARM site in Oklahoma, (Lenderink et al., 2004). This case is potentially difficult due to the non-

stationary character of the cloud variables.

The experimental model setup is described in section 4. The HIRLAM physics for parameterizing turbulence and convection is described in section 5. The emphasis is on the description of modifications to the convective parameterization.

The results for the different types of convective cases are presented and discussed in section 6. The role of different versions of turbulence and convection parameterization is investigated. It is shown that the modified convection scheme has a significant and positive impact on the BOMEX and EUROCS cases. Finally, section 7 provides some concluding remarks.

4   Experimental setup

The model setup is based on a column model of the physical parameterizations with specified dynamical forcing for the atmospheric prognostic variables. This means that both horizontal advection and subsidence effects can be described. This setup has previously been used in studies of the basic properties and performance of HIRLAM physics ,e.g. (Sass, 2001).

The ASTEX case and the BOMEX case have been studied systematically previously, and the forcing for the column models has been been available for several years. (Holtslag et al., 1998).

The ASTEX case has been computed for nocturnal conditions, that is, with no solar radiation switched on in the HIRLAM radiation scheme. Subsidence effects are included on the prognostic variables prescribing a linearly increasing subsidence velocity up to a height of 1500 m where the velocity of $7.5 \cdot 10^{-3} \mathrm{m} \cdot \mathrm{s}^{-1}$ is used. Above this height the subsidence is constant. The surface fluxes of sensible and latent heat are kept fixed in the default experiment, with prescribed fluxes equal to -12.4 $\mathrm{W} \cdot \mathrm{m}^{-2}$ and -30.6 $\mathrm{W} \cdot \mathrm{m}^{-2}$ respectively (negative fluxes are counted upwards).

Similarly a setup for the BOMEX case is available. Here the radiation tendencies or fluxes are completely specified. Again subsidence is specified by linear expressions, increasing from zero at the surface to $6.5 \cdot 10^{-3} \mathrm{m} \cdot \mathrm{s}^{-1}$ at a height of 1500 m. It then decreases linearly from 1500 m to zero at a height of 2100 m. The subsidence velocity is zero above this level. The combined temperature forcing due to radiation and advection (subsidence) is such that the net effect is zero above 2000m. For humidity a horizontal advection of dry air is specified $1.2 \cdot 10^{-8} \mathrm{kg} \cdot \mathrm{kg}^{-1} \cdot \mathrm{s}^{-1}$ in addition to the vertical advection from the specified vertical velocity. This horizontal advection below a height of 300 m decreases linearly to zero above a height of 500 m. Also in the BOMEX case the surface sensible and latent heat fluxes are kept constant at -9.5 $\mathrm{W} \cdot \mathrm{m}^{-2}$ and -153.1 $\mathrm{W} \cdot \mathrm{m}^{-2}$ respectively.

The forcing associated with the EUROCS case has been specified in the context of an international project where different column models were intercompared (Lenderink et al., 2004). In this case the forcing in both the atmosphere and at the surface is time dependent. A strong diurnal cycle is present in the surface fluxes. The latent heat flux at the ground is large in the middle of the day and reaches -500 $\mathrm{W} \cdot \mathrm{m}^{-2}$ which is considerably larger than the sensible heat flux at the same time -140 $\mathrm{W} \cdot \mathrm{m}^{-2}$

The present study is carried out with a rather high vertical resolution. 80 vertical levels is used, with 17 below 1000m, 5 between 1000m and 1500, 11 between 1500m and 3000 m, in total 33 levels below 3000 m. This is a high but feasible resolution for modern operational model systems. The experiments were run with a time steps of 150 s.

The column model enables a lot of diagnostic output and special output for specific cases. For the

present study it has been chosen to display similar type of output for both ASTEX, BOMEX and EUROCS to emphasize differences and similarities between the cases. Relevant vertical profiles are shown of parameters such as relative humidity, liquid water potential temperature, cloud cover, cloud liquid water, wind components and turbulent kinetic energy. These are displayed at the end of each model integration for a number of combinations of turbulence and convection parameterizations. For the EUROCS case also some time series are shown of cloud base height, cloud top height, maximum layer cloud cover and vertical mean turbulent kinetic energy below 900 hPa, respectively. Further details are given in section 6 as the results for the different experiments are presented.

5   The HIRLAM physics

Recent versions of HIRLAM physics are studied in the present report. The sensitivity of results to turbulence parameterization and convection parameterization is studied. The HIRLAM 7.1 physics code is used (see the code release notes on http://hirlam.org) The results of the latest experimental version of the cloud- and convection scheme is compared with the previous scheme used in HIRLAM 7.0.

5.1   Turbulence parameterization

The turbulence parameterization in HIRLAM combines 'turbulent kinetic energy' as a prognostic variable and a diagnostic length scale as a free parameter for the turbulence closure (Cuxart et al., 2000). The original lentgh scale, (Bougeault and Lacarrere, 1989) has been developed further (Lenderink, 2002). The scheme has , until recently, been a socalled 'dry' scheme (Undén et al., 2002). This scheme fails to describe adequately the turbulence in moist unstable cloudy conditions. Recently the scheme has been extended to diagnose moist unstable conditions and diffuses moist conservative variables, the total specific humidity and the liquid water potential temperature. The cloud condensate variable is reestablished from an approximate relationship using total humidity flux and liquid water temperature flux, and assuming saturated conditions inside clouds. The specific humidity tendency is then the difference between the tendency of total specific humidity and of cloud condensate. The algorithm supports both the 'dry' scheme and the 'moist' scheme.

5.2   Convection parameterization

The default convection scheme in HIRLAM is based on a moisture budget where the available moisture for convection ('moisture convergence') is distributed vertically between moistening on one hand (without previous condensation) and condensation on the other (with related latent heat release). The cloud condensate is distributed vertically by means of a separate function. This is relevant since condensed matter is not automatically precipitating out of the atmosphere. The vertical distribution functions depend on the cloud ascent model. This model is mentioned further in section 5.4. The cloud ascent model is not built on explicit mass flux computations but on an air parcel lifted and subject to classical mixing concepts with environmental air. The vertical extent of convection is determined by the level of non-buoyancy plus an entrainment layer simulating overshooting eddies. Fluxes of heat and moisture across the level of zero buoyancy is included to increase the realism of the model. The default cloud- and convection scheme is briefly described in a HIRLAM documentation (Undén et al., 2002). The modified convection parameterization has recently been described in an updated

documentation of the cloud- and convection scheme (Sass, 2007)

5.3 Modified convective cloud cover

The convection scheme to be compared with the 7.0 reference scheme contains a modified convective cloud cover.

The new convective cloud cover formulation is based on a piecewise rectangular probability function of total specific humidity. Only two boxes have nonzero probability which implies that the integrated probabilty over these two boxes must be 1. The box with low humidity (cloud free box) is confined between a minimum q_* and the grid box mean specific humidity $\overline{q}$. The other box is confined between the values of $q_s(T_c)$, the saturation specific humidity of a mean convective cloud temperature T_c and a maximum value q_{max} which may be computed on the basis of 3 governing equations, namely, the integrated probability (integrating to 1), an equation for grid box specific humidity based on the probability function, and finally an equation for the grid box cloud condensate. A solution for these equations (Sass, 2007) leads to a particular equation for the convective cloud cover f_{cv} [see (1) below]

Unlike previous formulations used with the present convection scheme the new formulation is applicable over the entire range of possible temperatures and humidities.

$$f_{cv} = 1 - \frac{2\left(q_s(T_c) - \overline{q}\right)}{2q_s(T_c) - \overline{q} - q_*} \tag{1}$$

In (1) $q_* < \overline{q}$ is the lowest occurring specific humidity which needs to be parameterized from other model variables. Currently the following parameterization is used for q_*

$$q_* = \overline{q}\frac{(1 - K_a\widehat{Q})}{(1 + K_b\frac{q_c}{q_s})} \tag{2}$$

In (2)

$$\widehat{Q} = min(\frac{\widehat{Q_a}}{Q_{00}}, 1) \tag{3}$$

The second term in the nominator of (2) involving K_a tentatively describes a small effect of moisture availability to the convective cloud. $\widehat{Q_a}$, constrained to be non-negative, is the vertical mean moisture supply to the convective cloud $(kg \cdot kg^{-1} \cdot s^{-1})$ through humidity advection and convergence.

$K_a = 2.5 \cdot 10^{-2}$, $K_b = 6.0$, $Q_{00} = 3.0 \cdot 10^{-8}kg \cdot kg^{-1} \cdot s^{-1}$

The denominator of (2) expresses a dependency on total specific cloud condensate q_c through the dimensionless parameter $q_c/q_s(T_c)$

The formulation of convective cloud cover expressed by (1) and (2) is well behaved for all values of the parameters since q_* is always less than $\overline{q}$, and $\overline{q}$ is always less than $q_s(T_c)$. Hence the cloud cover will always be non-negative.

It is seen that for small moisture availability which may be zero or negative plus a cloud condensate value going towards zero the fraction between nominator and denominator of (1) goes towards 1 , and hence $f_{cv} \rightarrow 0$.

On the other hand, for very moist conditions where $\overline{q} \to q_s$, with increasing values of cloud condensate q_c the cloud cover will approach 1, because the denominator will remain positive (although often small) while the nominator will approach zero for the assumed conditions.

5.4   Entrainment parameterization

The vertical extent of convection is determined by a classical buoyant parcel subject to entrainment with environmental air. Convection stops when the vertical velocity is estimated to become zero. The treatment of fractional entrainment automatically means that mixing of increasingly dry environmental air gives rise to less buoyancy of the parcel. A top entrainment layer is estimated to extend between the height when the parcel buoyancy becomes zero and the height when the vertical velocity becomes zero (Sass, 2007).

However, it is a challenge to parameterize the conditions for onset or triggering of convection. Intuitively the perturbations from grid box mean conditions, which may lead to convection, should depend on the intensity of subgrid scale motions and on the model resolution. These effects are currently parameterized in terms of the subgrid scale turbulent kinetic energy E and a dimensionless grid size D_* according to (4) and (5).

The parcel starts with a parameterized excess temperataure T_x and specific humidity q_x

$$T_x = \frac{K_{x0} \cdot E}{K_{x1} + K_{x2} \cdot (D_*)^{0.50}} \tag{4}$$

$$q_x = \overline{q}\Big(1 + K_{x3} \cdot E \cdot (D_*)^{-0.25}\Big) \tag{5}$$

In (4) and (5) $K_{x0} = 0.75\text{s}^2 \cdot \text{m}^{-2}$ K_{x1}=0.89 K^{-1}, $K_{x2} = 0.079\text{K}^{-1}$ and $K_{x3} = 0.024\text{s}^2 \cdot \text{m}^{-2}$

These constants have been determined to give satisfactory results with current physics and the entrainment formulation described below.

Significant amplitudes of initial perturbations of temperature and specific humidity are to some extent supported by observational studies. Emanuel (1994, page 198) mentions that large temperature and humidity variability on small scales has been observed in connection with non-precipitating cumuli.

In (4) and (5) D is the model grid size, and D_* is a dimensionless parameter

$$D_* = \frac{D_{cv}}{D} \tag{6}$$

In (6) D_{cv} is a characteristic horizontal scale (D_{cv}=4000 m) for a cloud resolving model. Below this scale a significant part of convective clouds starts to be resolved by the atmospheric model. The perturbations expressed in (4) and (5) will approach zero in the ultimate limit of D $\to$ 0. However such convergence should be quite slow in view of the possible small sizes of clouds down to 100m or smaller for shallow convective clouds in the low troposphere.

The modified entrainment formulation may be written

$$\epsilon_e = \left(K_{\epsilon 0} + \frac{K_{\epsilon 1}}{Ri_*}\right) \cdot D_* \cdot Z_*^2 \qquad (7)$$

The first term $K_{\epsilon 0}$ in the brackets of (7) is a basic entrainment parameter. The second term describes an effect of wind shear. Z_* is a dimensionless height defined as

$$Z_* = \frac{z}{K_{\epsilon 2}} \qquad (8)$$

The current values of the constants are $K_{\epsilon 0} = 5.0 \cdot 10^{-4} \mathrm{m}^{-1}$, $K_{\epsilon 1} = 7.5 \cdot 10^{-4} \mathrm{m}^{-1}$ and $K_{\epsilon 2} = 2250 \mathrm{m}$

In (7) D_* as described above expresses a classical type of cloud parcel (bouble) entrainment inversely proportional to cloud diameter. (Malkus and Scorer, 1955; Scorer, 1957) Currently D_* is constrained to be no less than 1 which means that the parameterization becomes active for parameterized convection below the grid size threshold of D_{cv}. It means that the cloud parcel mixing with environments becomes increasingly efficient for smaller grid sizes. This gradually tends to switch off deep convection parameterization as should be expected.

The inverse radius type of relationship has some support in observational studies e.g., (McCarthy, 1974). This study is concerned with relatively small cumulus clouds and hence supports the suggestion of the present scheme that the inverse radius relationship be applied to small clouds. The studies of Mc Carthy leads to a fractional entrainment ϵ_b of a cloud with radius equal to R_b: $\epsilon_b \approx 0.6/R_b$. Translating the basic entrainment parameter $K_{\epsilon 0}$ to this relation gives a cloud size of radius 1200 m indicating that this basic coefficient is of a right order of magnitude for cumulus convection. However, uncertainty remains on how to parameterize entrainment rate as a function of grid size and height in an atmospheric model.

For example, the inverse radius relationship is not realistic for large clouds where other entrainment mechanisms are important such as mixing of dry air through cloud tops down to significant depths of the cloud. A clear documentation of this effect goes back to 1979 (Paluch, 1979). Measurements of liquid water content in cumulus clouds as a function of height indicates increased entrainment with increasing height (Pruppacher and Klett, 1978), page 495, rather than decreasing entrainment indicated by an inverse radius relation for expanding clouds at higher levels. To describe an increased entrainment with height the term Z_*^2 is included in (7). The power of two gives good results on the investigated data sets for shallow convection but is otherwise not based on theoretical arguments. Also this formulation leaves it open at which height a maximum entrainment should be reached. Currently Z_* is constrained to be no more than $\sqrt{2}$ giving $K_{\epsilon 0} \cdot Z_*^2 \leq 1.0 \cdot 10^{-3}$.

Also a dependency of a Richardson number Ri_* is a part of the entrainment formulation (Sass, 2007). It may be argued qualitatively that increasing wind shear gives rise to more mixing of the convective cloud with the environments. The significance of wind shear on the evolution of convective clouds has been mentioned by others, e.g. (Cotton and Triopli, 1978)

5.5 Moistening parameter

The moistening parameter β is parameterized accoording to the following formula

$$\beta = 1 - \frac{1}{1 + \sqrt{\frac{D_{cv}}{D} \cdot \left(\overline{\frac{q_c - q_e}{K_H}}\right)}} \tag{9}$$

This parameter expresses the fraction of the converging humidity on grid scale that is part of parameterized convective activity without condensing to cloud condsensate. In (9) a dependence of resolution is introduced through the square root of D_{cv}/D. Qualitatively such dependency should be expected.

For coarse mesh models small values of β should be expected due to the possibility of intensive unresolved mesoscale convective systems. It cannot be exluded that the humidity going into convection, for periods of time, can exceed the amount of humidity transfered to the grid column due to advection and convergence. However, the present formula only describes values between zero and 1.

For a small grid size one may be guided by the observational studies , e.g. (Braham, 1952). He analysed extensive data on small thunder storms in Florida and Ohio and found that for these clouds approximately 60 % of the water vapor inflow condenses while the rest leaves the storm without phase change. This indicates that the value of the moistening parameter β on model grid scales of, say 10 km, will not be much larger than 50%. The term $\overline{q_c - q_e}$ in the denominator of (9) describes the vertical mean of the specific humidity between cloud and environment over the convective cloud. It is scaled by the humidity constant $K_H = 1.50 \cdot 10^{-2} \mathrm{kg} \cdot \mathrm{kg}^{-1}$. which currently to some extent is a tuning constant for a given model.

6 RESULTS

6.1 ASTEX stratocumulus case

The model is integrated over 24 hours for different choices of turbulence and condensation scheme. The vertical model profiles at +24 hours are shown in Fig.1 a-f and Fig.2 a-f. The parameters are, respectively, relative humidity (1a, 2a) , liquid water potential temperature (1b, 2b), cloud cover (1c, 2c), cloud water (1d, 2d), wind profile components (1e, 2e) and turbulent kinetic energy (1f, 2f). Results for the 'dry' turbulence scheme plus condensation without a convection scheme are named 'cbrd-noc', the 'moist' turbulence scheme without a convection is named 'cbrm-noc'. Finally, the moist scheme plus the current and new convection schemes are called 'cbrm-cv' and 'cbrm-cvnew' respectively. The experiments apply to nocturnal conditions, that is, with the model's radiation scheme switched on, but with no solar radiation switched on. The surface fluxes of sensible and latent heat were kept fixed in default experiments using -12.4 $\mathrm{W} \cdot \mathrm{m}^{-2}$ and -30.6 $\mathrm{W} \cdot \mathrm{m}^{-2}$ respectively (fluxes positive in downward direction).

Overview articles of this field experiment carried out in June 1992 are available in the litterature (Bretherton and Pincus, 1995; Albrecht et al., 1995). The dataset for 1D-tests is an idealization of the period 12-13 June where the statocumulus remained solid but was in a deepening phase with significant entrainment rates w_e at cloud top. All figures (1a-1d) and (2a-2d) reflect in some way the presence of the vertical cloud structure.

The entrainment velocity is the velocity of the cloud top due to mixing of dry air above cloud into the cloud in the absence of a subsidence velocity w_s. To get actual movement w_t of the cloud top the subsidence must be taken into account: $w_t = w_e + w_s$ (where subsidence is counted negative). Various estimates of w_e have been made from observational data sources (Bretherton et al., 1995). There is a significant scatter in the results. A first method used ECMWF synoptic scale analyses including observed rate of change of inversion height. This method gave $w_e \approx 0.9 \mathrm{cm} \cdot \mathrm{s}^{-1}$. A second method was calculating the entrainment drying as a residual in the water budget of the mixed boundary layer air

column giving $w_e \approx 1.0 \mathrm{cm \cdot s^{-1}}$ A third method was based on ozone measurements above and below the cloud top giving $w_e \approx 0.6 \mathrm{cm \cdot s^{-1}}$. Finally, a study of aircraft data during the first night between 12 and 13 June (Duynkerke et al., 1995) was leading to entrainment values as high as $1.3 \mathrm{cm \cdot s^{-1}}$. The mean of the 4 estimates equals 0.95 $\mathrm{cm \cdot s^{-1}}$ The values derived from the present study were computed by keeping track of cloud top derived as a transition to a non-zero fractional cloud cover in excess of 1 %. Table 1 shows the simulation results for the time mean of w_t, w_e and w_s.

Table 1 :
Time mean entrainment velocities w_e, subsidence w_s and total cloud top movement w_t for the different experiments forced from standard ASTEX data $(\mathrm{cm \cdot s^{-1}})$

Experiment	We	Ws	Wt
cbrd-noc	0.33	-0.33	0.00
cbrm-noc	0.82	-0.43	0.39
cbrm-cv	0.99	-0.49	0.50
cbrm-cvnew	1.00	-0.50	0.50

It is seen from the table that all experiments except 'cbrd-noc' produce mean entrainment rates over 24 hours within the range of estimates based on observations. The combined physics including a convection scheme produce somewhat higher entrainment rates than 'cbrm-noc'. The failure of 'cbrd-noc' is related to the fact that the scheme cannot increase turbulence in the cloud layer. This is, for example, reflected in the substantially decreasing liquid water potential temperature (θ_l) towards the cloud top, caused by strong radiative cooling at the top. A slight decrease of θ_l is also seen in the other more successful runs. A similar small 'dip' in θ_l has been found in other studies of stratocumulus using higher order turbulence schemes (Chen and Cotton, 1987; Bougeault, 1984). Whether this small decrease of θ_l is realistic may be questioned. It may be caused by an excessive radiative cooling rather than a deficiency of the turbulence parameterization.

All simulations are successful from the point of view that the cloud cover remains unbroken during the simulation period. The shape of the cloud cover profile is better preserved for 'cbrm-noc' compared to 'cbrm-cvnew' and 'cbrm-cv'. These cloud decks have slightly thickened in vertical extent which may seem surprising at first since dryer air is mixed into the cloud. However, cloud thickening is non uncommon in the context of stratocumulus entrainment (Randall, 1984). For 'cbrd-noc', however, the cloud cover profile indicates som cloud thinning because of a higher cloud base. This is to some extent contradictory to the fact that small amounts of cloud condensate extends towards the surface (fig. 2d) - a feature which is considered unrealistic. The cloud parameterization of 'cbrd-noc' is not classifying this as a cloud because the relative humidity is not high enough to parameterize stratiform clouds. The cloud 'thinning' seems in this case related to the precipitation release which is 1.3 mm during 24 hours for 'cbrd-noc'.

For the other cases entrainment has probably contributed to cloud thickening. In addition, precipitation release was smaller in these runs. The simulation 'cbrm-noc' released 0.8 mm of precipitation, and the smalllest precipitation was obtained in the runs using convection schemes releasing only 0.4 mm ('cbrm-cv') and 0.5 mm ('cbrm-cvnew'). In the ASTEX data drizzle was observed to be quite varying in time. The estimated average precipitation intensity was around 1 mm/day (Bretherton et al., 1995).

Fig.1e and Fig.2e show the geostrophic wind components $U_g = -2 \mathrm{m \cdot s^{-1}}$ and $V_g = -10 \mathrm{m \cdot s^{-1}}$ which are constant with height. This results in corresponding weak variations of the actual wind profiles in the figures. The turbulent kinetic energy (TKE) as shown in Fig.1f and Fig.2f is another indicator of the transports of energy, humidity and momentum up to the top of the stratocumulus layer.

It is beyond the scope of the present paper to analyse the TKE budget. It is however clear that the runs producing most entrainment are characterized by the largest TKE values which tend to increase up through the cloud layers towards the cloud top where the turbulent exchanges with the dry air above will be enhanced. The moist turbulence scheme has the ability to generate more TKE near the cloud top through the buoyancy generation term. On the contrary, it is clearly seen that the dry turbulence scheme is characterized by decreasing TKE up through the stratocumulus cloud.

It may be concluded that the different parameters shown in figures a-f give a coherent picture of the different simulations which have been run with fixed surface fluxes. One may ask what happens if the surface fluxes are allowed to evolve freely. Such experiments (not shown) exhibit a similar cloud evolution, but the decreasing relative humidity near the surface in all simulations (Fig.1a and Fig.2a) is less pronounced.

Since the ASTEX experiment is related to a transition of stratocumulus to cumulus it is of interest to carry out some additional simulations investigating such possible transitions. Fig 3 shows the results of 3 such cases. 'SUB' signifies an experiment run over 30 hours where the prescribed subsidence vertical velocity profile is multiplied by a factor of two. 'SUBTS' applies to similar conditions as 'SUB' but specifies in addition that the sea surface temperature (SST) increases linearly with time from the initial value of 16.9 °C to 23.2 °C after 30 hours (5 °C/day). This simulates an effect of flow towards higher SST. Finally 'DRY' is the result of the original SST and subsidence but with the nearest 6 model levels above cloud top (total depth of about 550m) having a $1.0 \ \mathrm{kg \cdot kg^{-1}}$ initial specific humidity instead of the 7- 8 $\mathrm{kg \cdot kg^{-1}}$ higher humidity of the original experiment. In relative humidity this corresponds to a drop from 100 % at cloud top to a mean value of about 10 % of the dry layers.

The results of Fig.3 are quite interesting. Although it is not possible to compare with observations for these simulations the results are qualitatively what could be expected with a realistic model. In the first simulation 'SUB' we see an effect of increased subsidence. Since increased heating of the cloud is involved due to the increased adiabatic heating process one might expect the cloud to dissolve. The importance of subsidence for stratocumulus evolution has been stressed by others, (Weaver and Pearson, 1990). The characteristic time scale involved is typically 1 day. This is consistent with 'SUB' where clouds start to breakup after 21 hours. The fractional cloud cover decreases over a period of about 6 hours to a small amount. It is noted that putting the subsidence to zero instead of a doubling leads to a larger lifting of the cloud deck due to entrainment and, as expected, no breakup of the clouds.

In 'SUBTS' we see that the stratocumulus deck starts to break up after about 13 hours instead of 21 hours in 'SUB'. The increasing SST by about 2.7 °C is giving rise to this difference. A transition period of almost 3 hours with decreasing cloud amounts leads to a local minimum of a little less than 40 %. Afterwards a slowly increasing cloud cover takes place to almost 70 % by the end of the simulation period. In this case a shallow unstable cumulus convection regime is established with convective clouds between 700 m and 900 m and a more significant dry inversion above due to the more pronounced subsidence compared to the reference experiment. The important message is that changing SST by a rather modest amount (2.7 °C) leads to a significantly different forecast.

Finally, in 'DRY' the dry layer above the stratocumulus deck (together with the reference subsidence leads to a rapid breakup of the cloud deck. The transition starts shortly after the first hour of simulation. The possibility of rapid breakup of stratocumulus clouds has been mentioned by many authors, e.g. in the context of the theory of cloud top entrainment instability (Deardorff, 1980). According to this theory rapid cloud breakup, e.g. within less than 1 hour can result as a result of mixing dry air into stratocumulus at the cloud top. In the present case the basic transition towards a low level takes place during half an hour. It is noted that a significantly smaller depth of the dry layer prevents the

cloud layer from breakup.

These simulation results clearly indicate the challenges of cloud cover forecasting when stratocumulus is involved because of the sensitivity to initial conditions and forcing. In addition, the wind shear can be of importance in some situations (Duynkerke and Driedonks, 1988)

6.2 BOMEX shallow cumulus case

This case is a true shallow cumulus case. It represents quasi steady state conditions for the tropical trade winds. The data originates from the tropical sea ($\approx 13 - 17°$ N), ($\approx 54 - 59°$ W) close to Barbados. The BOMEX field experiment has been described by Esbensen (1974).

The main importance of this experiment is to demonstrate that the moist physics can adequately describe the heat and moisture transports up through the the lowest 2 km of the atmosphere while keeping the fractional cloud cover at a low amount. Otherwise the model will produce a too moist boundary layer with too dry air higher up due to heating and drying from subsidence. Moreover, the model must not generate any substantial precipitation from the convective clouds.

The simulation results are shown in Fig.4a-f and Fig.5a-f. The simulation period is 7 hours which was used in the LES to obtain quasi-stationary conditions. Therefore the initial profiles shown in the figures and the cloud cover profile ('cld-bomex') are indicators of the desired results. The nomenclature is similar to that described for ASTEX.

It is very clear that the experiments 'cbrd-noc' and 'cbrm-noc' with no convection scheme switched on fail to describe the structure of the lowest 2 km of the atmosphere properly. The relative humidity becomes too high in the lowest km of the atmosphere. The cloud cover is much excessive, and the liquid water is also too high. The simulated max. cloud amounts from LES are between 5 % and 7 %. This amounts are to be compared with 50 % obtained with 'cbrd-noc' and almost 75 % with 'cbrm-noc'. The effect of moist turbulence in this case is to move moisture to a higher level as compared to the dry version. In both cases the result is unrealistic. The simulated cloud water from LES is very low for BOMEX (typically $10^{-6} - 10^{-5} \mathrm{kg} \cdot \mathrm{kg}^{-1}$). When the default convection scheme 'cbrm-cv' is switched on the relative humidity profiles improve a lot (Fig.4a and Fig.4c). The cloud cover is still somewhat excessive and so is the cloud water, but mainly between 700m and 1000 m. When the new convection scheme is used both the relative humidity, the cloud cover and the cloud water are substantially improved compared to the default convection. In fact the cloud cover profile is in remarkably good agreement with observations. The cloud top (where the cloud cover becomes less than 0.5 %) is at approximately 1800 m in excellent agreement with observations and LES.

Fig.4e and Fig.5e show that geostrophic wind is decreasing with height for BOMEX. The cross isobar angle close to the surface remains relatively low (12 °) even though the tropical latitude. Again the TKE show different behaviour for the simulations using convection schemes compared to those with only turbulence parameterization for the vertical transports. In all schemes the turbulence is basically limited to the lowest 1200 m of the atmophere. While the TKE steadily decreases with height in the runs without convection (except between 700m and 900m in 'cbrm-noc') the runs based on convection schemes have a higher TKE and a clearly defined maximum in the lower part of the convective cloud. This peak is especially pronounced with the new convection scheme. The reason for this is not entirely clear but it illustrates the interaction between the convection scheme and turbulence scheme.

6.3 EUROCS cumulus case

This case is devoted to study the diurnal cycle of cumulus over land at mid latitude summer conditions. More specifically the initial conditions and the forcing for the LES represent an idealization of observations from 21 June 1997 in the area of the great planes in Kansas and Oklahoma. The design and problems associated with the LES tests are documented by Brown et al. (2002). The associated column model tests of an international intercomparison study are described in Lenderink et al. (2004).

It turned out to be rather difficult to construct appropriate initial conditions and forcing for the model studies. In fact, a direct comparison to observations is difficult due to these problems (Brown et al., page 1081). As a consequence of the compromises made in the study it turned out to be difficult to get good agreement with all aspects of the various observations. For example, The simulated cloud top height of the LES were too low during the morning after the onset of convection. Moreover, the cloud bases from the simulations were generally too low by 200m -500m. The default settings of the LES was such that the microphysics (precipitation release) was switched off. - Allowing precipitation release in the present simulation for 'cbrm-cvnew' gave less than 0.1 mm accumulation which is a quite satisfactory result.

However, default settings for the present column experiments are in accordance with conditions used for LES. As a consequence, the column model 'inherits' the problem that a direct comparison to observations is dificult, and the quality needs to be assessed primarily from the comparison with LES.

Fig.6 a-f show the results for the vertical model profiles after 10 hours of integration. The results are valid for mid afternoon local time. The model was run up to +15 hours including also the evening. Fig.7a-b show the time evolution of cloud base height and cloud top height respectively. The spread interval from LES are shown (see figure text). Fig.6c similarly shows the evolution of cloud cover in the 1D simulations and in LES. The maximum cloud cover from all model levels is shown. Fig.7d shows the time evolution of the vertical mean TKE below 900 hPa for the different experiments. Except for Fig.7d including the results of 'cbrd-noc', Fig.6 and Fig.7 only show the experiments using the 'moist' turbulence scheme.

The most remarkable and illustrative results are presented in figure 6a showing the 10 hour relative humidity profile. The new convection scheme manages to produce very good agreement with LES. The other convection scheme is too dry beteen about 1300m and 2100m and somewhat too moist below 900m. The simulation without a convection scheme exhibits serious problems since it is much too dry above 1700 m, and too humid at lower levels. The cloud cover is also excessive (Fig.6c). None of the 1D simulations manage to produce a very precise agreement of cloud cover with LES at the particular time shown. However, the new convection scheme reproduces better the characteristic decrease of cloud cover with increasing elevation.

The paper of Brown et al.(2002) does not present any results for cloud water. However, from Lenderink et al.(2004) it may be concluded that the 1D simulation results of Fig.6d give more cloud water than seen in the LES. This is typical for the 1D model results as presented by Lenderink et al.(2002). The reason for this difference is not completely clear, but may be related to the time scale assumed for evaporation of cloud water.

Fig.6e shows that the geostrophic wind is assumed constant in this experiment ($10 \, \text{m} \cdot \text{s}^{-1}$). It is noted that the model derived surface cross isobar angle in this case is 27 °. Fig.7f shows that the TKE at this time is very similar in the two runs using convection parameterization. It is seen that a significant level of TKE extends higher up in the run 'cbrm-noc'. This may be explained by the cloud cover and relative humidity profiles of Fig.6a and Fig.6c. It may be expected that the moist turbulence scheme generates a significant level of TKE near the cloud top around 1500m of this simulation (buoyancy

generated TKE).

Fig.7 a-b show that the simulated cloud base and cloud top height for the new convection scheme is in rather good agreement with LES. The cloud base of 'cbrm-cvnew' tends to be slighty higher than the values from LES which is in fact in better agreement with observations from a micro-pulse lidar and from a ceilometer. Also the 1D simulation describes a more rapid rise of the cloud top which is in better agreement with observations. However, because of the experimental design, it is not possible to put much emphasis on direct comparisons with observations.

It is seen from Fig.7a-b that the old convection scheme is too late with the onset of convection by more than an hour for this case. This result is strongly influenced by the assumptions related to perturbations and entrainment formulation for the convective cloud model. In Fig.7c it is seen that for the new convection scheme the triggering and the cloud amount in the first part of the simulation is is in good agreement with LES. Both schemes have to some extent problems to dissolve the clouds in the evening. The same problem is typical for the 1D model simulations of Lenderink et al. (2004). It appears that the conditions during evening are quite challenging, because the atmosphere remains rather unstable and moist where the convection has been active earlier in the day. In addition, the simulation specifies a rather high evaporation during most of the evening. These conditions imply that many models would tend to continue to diagnose convection in the evening.

Finally Fig.7f shows the vertically mass averaged TKE below 900 hPa as function of time. When such averaging is done we see that the differences between the different model simulations are more modest. Since the generation of TKE is much influenced by the vertical static stability of the planetary boundary layer one may expect a clear diurnal cycle of the vertical average TKE, with increasing values in daytime. This feature is clearly reproduced in the figure.

7   Concluding remarks

Shallow convection has been studied in a 1-dimensional column model with HIRLAM physics and appropriate forcing. The results indicate clearly that a traditional turbulence scheme combined with microphysics without a convection scheme is not suitable in general for describing the vertical transports of energy and humidity in shallow convective conditions. However, for a humid boundary layer with stratocumulus a moist turbulence scheme such as the existing HIRLAM one does a rather good job to describe the cloud evolution.

For the ASTEX case the entrainment rate at the cloud top agrees with observational estimates, both when the combined physics are used and when the moist turbulence scheme is used alone. The combined scheme produces somewhat higher entrainment rates. The vertical structure of cloud humidity and temperature is well described except when the 'dry' version of the turbulence scheme is used. In the latter case the liquid water temperature drops considerably near cloud top, and the cloud water extends too much at low levels towards the surface.

The liquid water potential temperature, expected to be quasi-constant in the cloud deck in reality, also exhibits a slight decrease near cloud top in the versions including the moist turbulence scheme and convection. This feature also known from other modeling studies of stratocumulus may be related to excessive radiative cooling in a shallow layer near cloud top. This cooling due to radiation is hard to compensate completely by the convective condensation processes.

The specific liquid water increases almost linearly with height and is in reasonable agreement with

observational estimates. The cloud deck remains unbroken in the reference simulation in accordance with observations.

The sensitivity experiments show qualitatively what can be expected when varying the subsidence, the SST and the humidity profile. It highlights the challenge of cloud cover prediction and emphasizes the likely importance of analysing correctly the initial state of the atmosphere and the surface.

The BOMEX and the EUROCS cases are genuine cases for shallow cumulus since smaller cloud amounts well below 100 % are involved. The new convection parameterization has given improved and very good results for the relative humidity profiles when compared to the reference results of LES. For BOMEX the new scheme also gives very good agreement with the LES cloud cover profile. In addition, the simulated very small values of specific cloud water is also found in LES. The simulated cloud cover and cloud water of the older version of the convection scheme verify poorer against LES.

The EUROCS case is a special challenge, partly due to the non-stationarity. The time of onset of convection is realistic in the new convection scheme at the resolution parameterized (5 - 10 km grid size). The old scheme is too late at activating convection for this case. The general level of cloud cover is in fair agreement with LES, but both schemes have to some extent problems to dissolve clouds towards the end of the simulation. This problem is typical for the 1D simulations of different model systems, as presented by Lenderink et al.(2004). Also the cloud water of 1D-simulations for this case appears to be larger than the LES counterpart. These aspects of the EUROCS case should be addressed in the future.

The simulated cloud base and cloud height with the new convection scheme is in rather good agreement with LES and also with observations related to the experiment.

A feature of operational 3-dimensional HIRLAM-systems in the past has been an overprediction of small precipitation amounts. The cases studied here show no signs of such overprediction due to the physical parameterizations. For BOMEX no precipitation is reaching the surface. For EUROCS less than 0.1 mm reached the surface during the simulation period when allowing precipitation release in the simulation.

In order to follow up the present study it is natural to do, on one hand, a comprehensive set of experiments in a 3-dimensional model version for grid sizes above the scale of D_{cv}. This set of experiments will focus on grid sizes of 5 - 10 km in view of the current operational model resolutions. The results of the present study indicate that the parameterizations will give quite realistic results for relative humidity and precipitation for clouds in the lowest 3 km of the atmosphere. However this needs to be confirmed in 3-dimensional model studies of different cloudy situations and for longer time periods. Some tuning aspects of precipitation release might turn out to be necessary for a given model system to get near optimal results. In addition, deep clouds have not been studied. Also clouds at low temperatures involving ice microphysics have not been included in the present study.

A second step would be to study the model at very high resolution using a grid scale below D_{cv}. This will allow to study how the convective precipitation decreases due to resolved scale dynamics and due to increased entrainment of the parameterized convective clouds as a result of the inverse grid scale dependency of entrainment. The latter experiments should preferably be done in a non-hydrostatic model in order to produce realistic vertical velocities and forcing to the condensation processes. In such experiments the precipitation species should preferably be fully prognostic variables in the general case, with realistic fall velocities relative to the surrounding air.
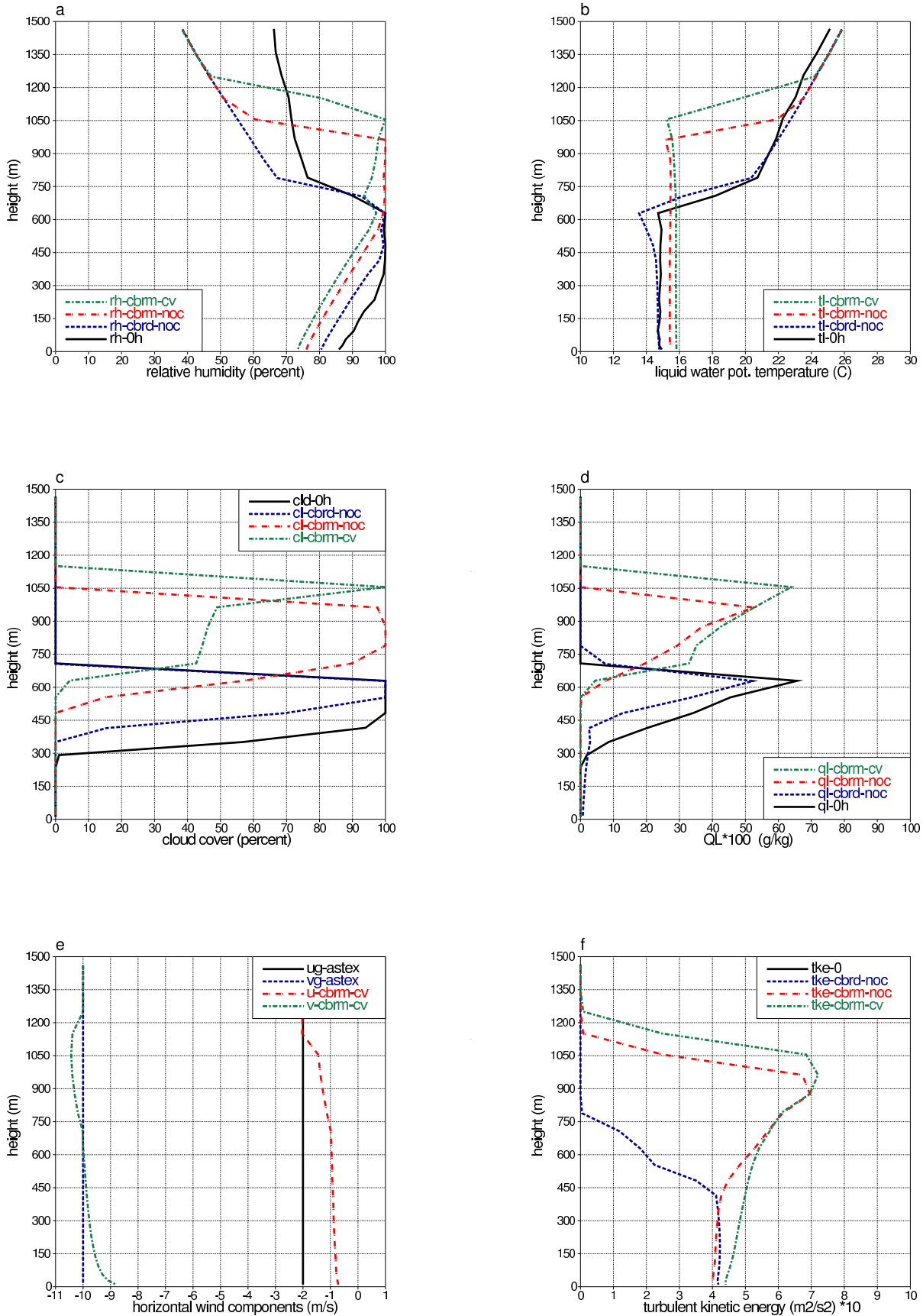
Figure 1: Vertical instantaneous profiles at 24 hours for ASTEX simulation with standard forcing (see text) -In the figures '0h' means intial conditions, 'cbrd-noc' means dry turbulence scheme with no convection scheme, 'cbrm-noc' signifies moist turbulence scheme without convection and 'cbrm-cv' means moist turbulence scheme plus HIRLAM-7.0 convection scheme - a) relative humidity profiles, b) liquid water potential temperature, c) cloud cover , d) specific liquid water scaled by a factor of 100, e) geostrophic wind and model's wind components, f) the turbulent kinetic energy profile scale by a factor of 10.
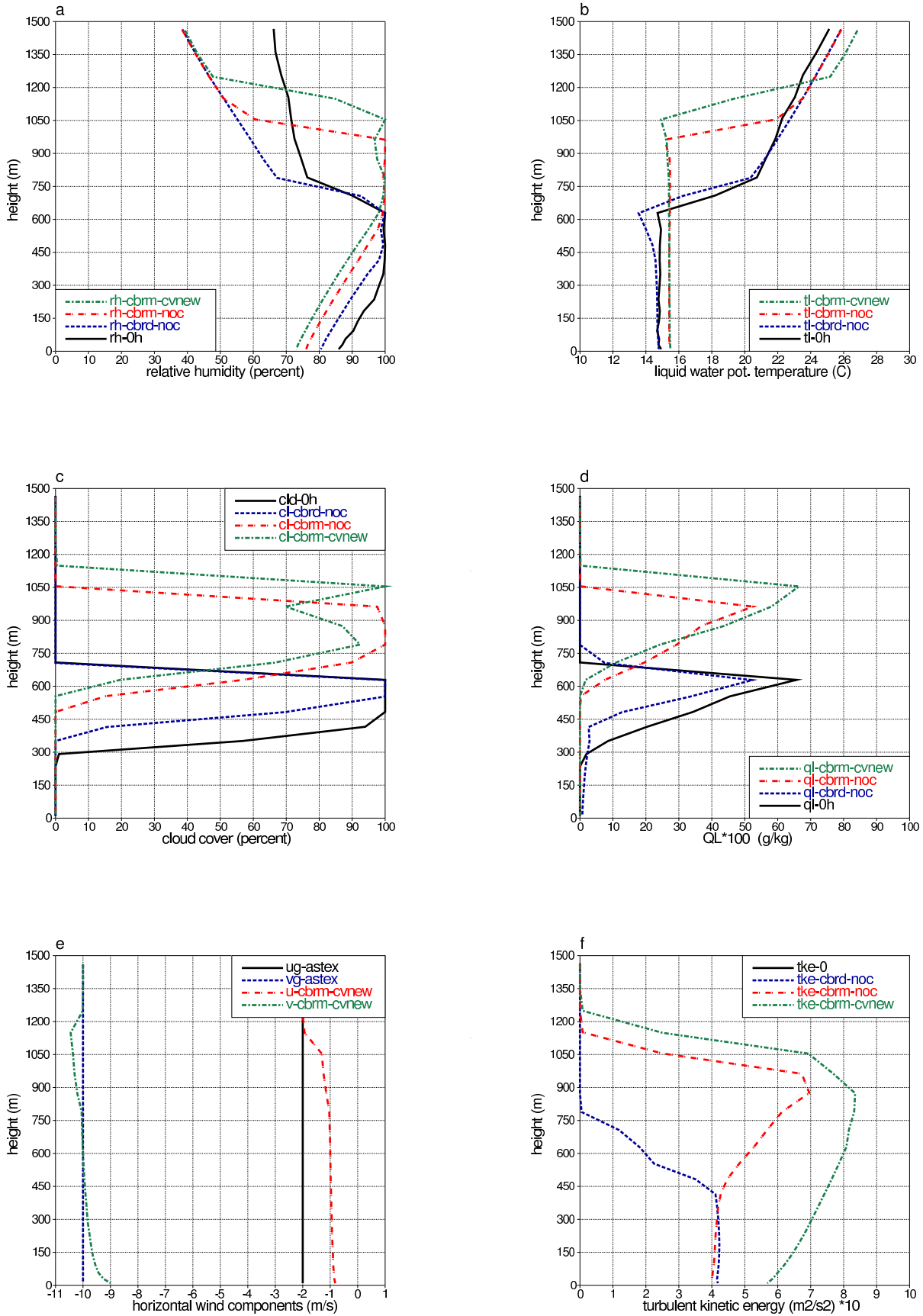
Figure 2: As Fig.1, but the HIRLAM 7.0 convection scheme is replaced by the new convection scheme as described in section 5. 'cbrm-cvnew' signifies new scheme. Curves for the other schemes are repeated to facilitate comparisons.
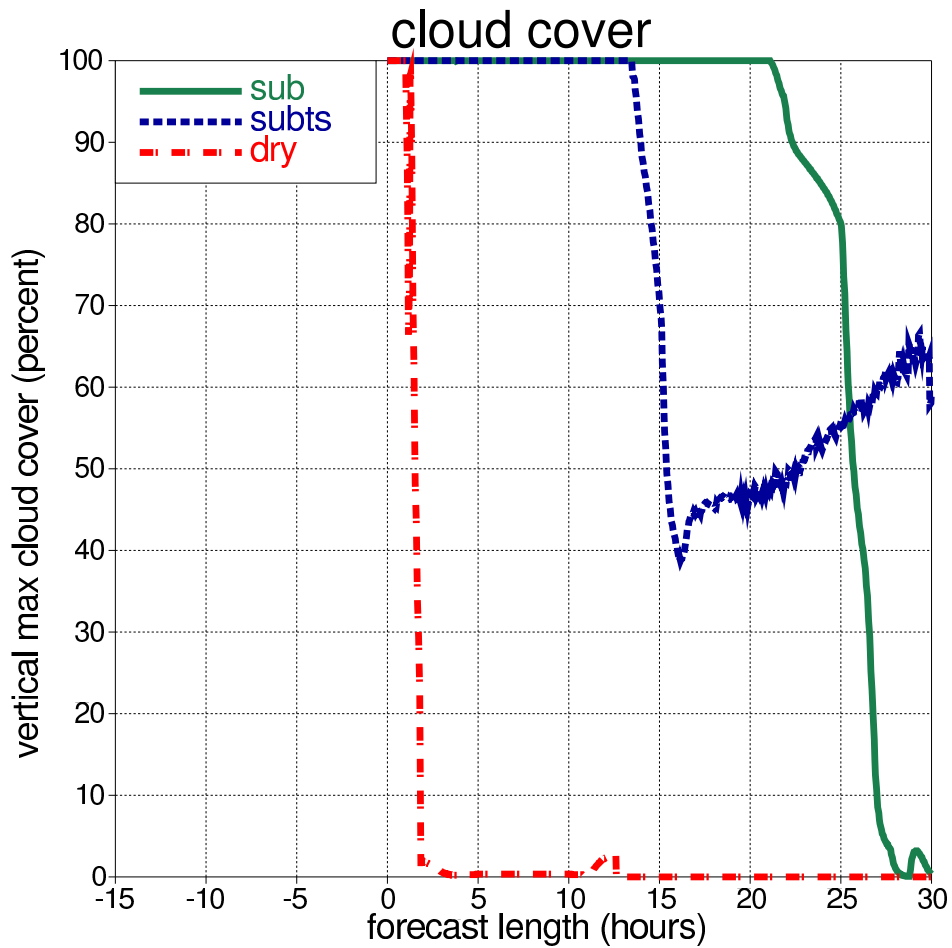
Figure 3: Simulations of stratocumulus breakup. Simulation period is 30 hours. Shown is the maximum fractional cloud cover of the model levels. 'DRY' signifies a modification due to the substitution of dry air (about 10 % relative humidity) in 6 model levels above cloud. 'SUB' applies to a doubling of the subsidence velocity and 'SUBTS' prescribes conditions as 'SUB' plus a linearly increasing SST as a function of time (5 K/day).
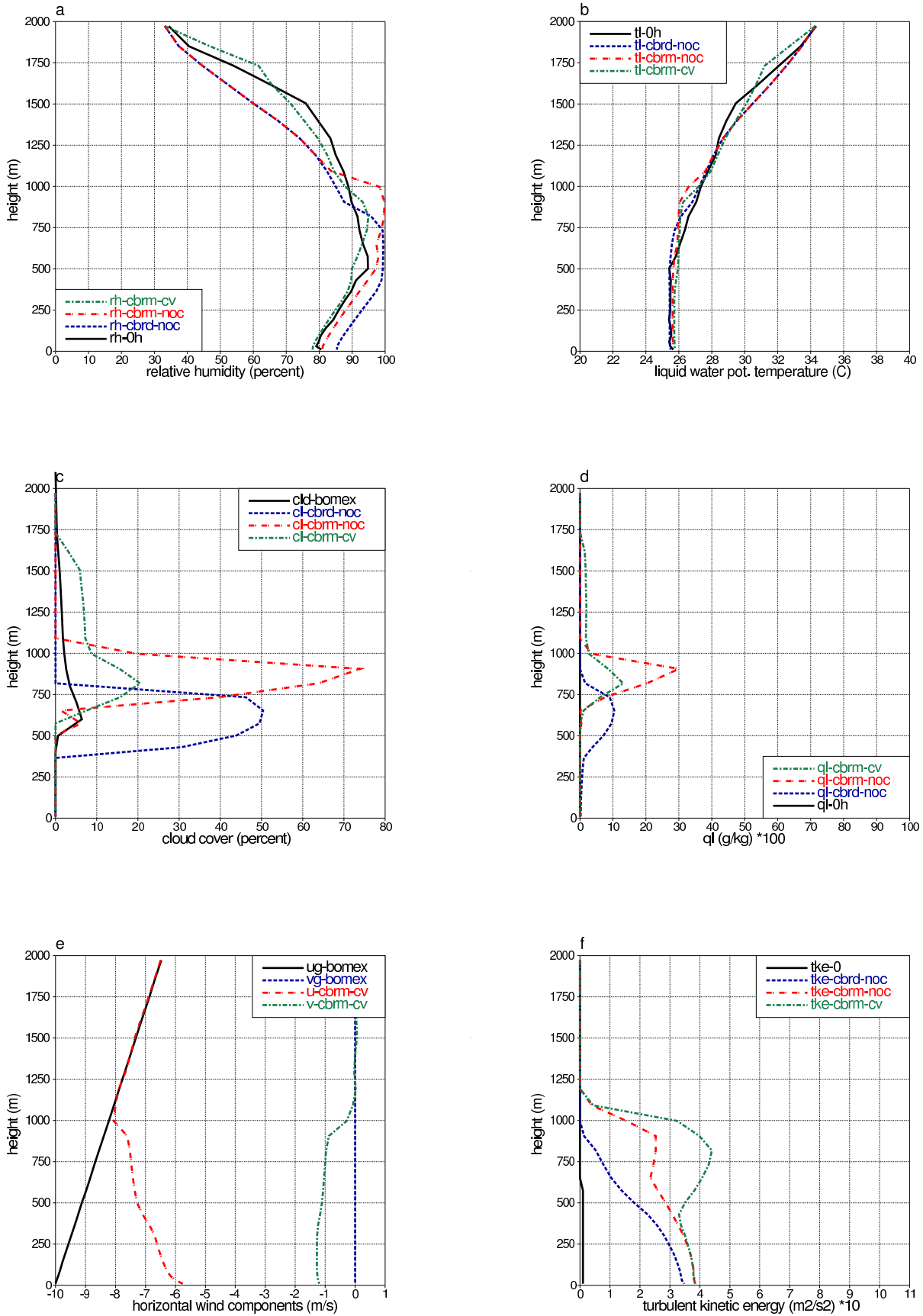
Figure 4: Vertical profiles for BOMEX tradewind cumulus case. The simulation parameters shown and the nomenclature are the same as in previous figures. The simulation time is 7 hours to compare with results of LES. 'cld-bomex' signifies a cloud cover profile derived from LES.
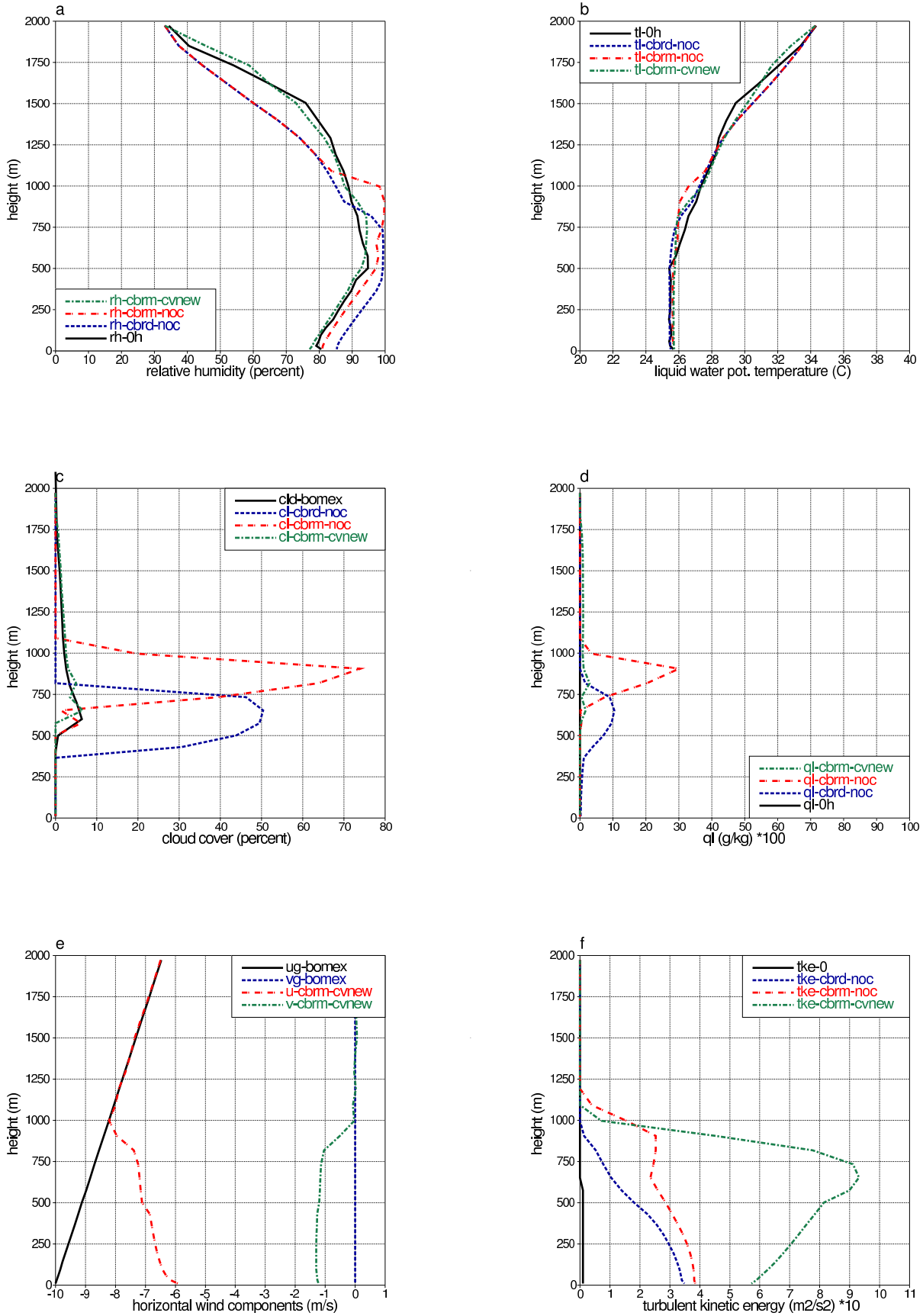
Figure 5: Vertical profiles for BOMEX tradewind cumulus case. The simulation parameters shown and the nomenclature are the same as in previous figures. The simulation time is 7 hours to compare with results of LES. 'cld-bomex' signifies a cloud cover profile derived from LES. Results of 'cbrm-cvnew' are replacing 'cbrm-cv'
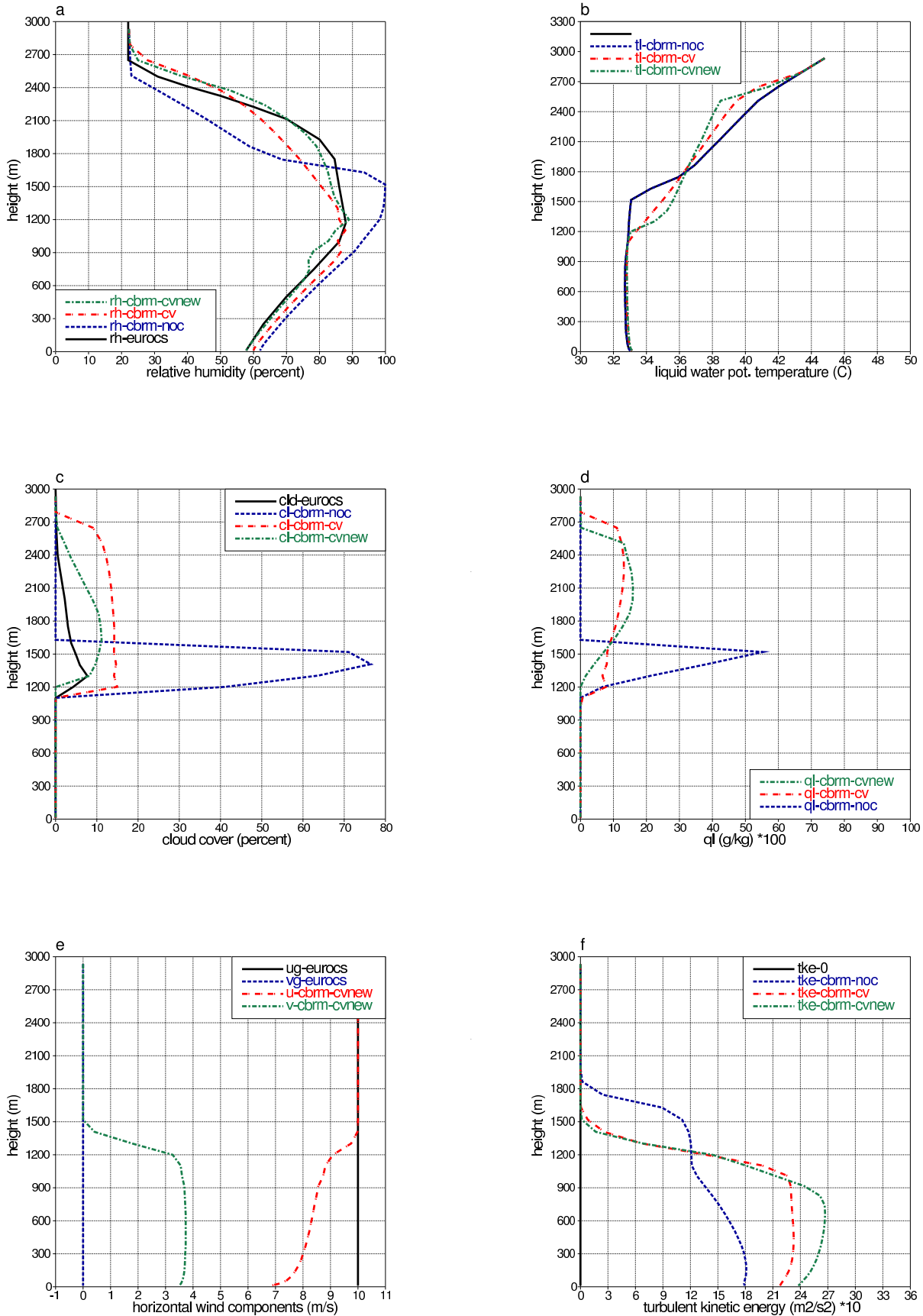
Figure 6: Results for the EUROCS shallow cumulus case. Vertical profiles at +10 hours (21.30 UTC) of the same parameters as shown in previous figures. The nomenclature is unchanged. 'rh-eurocs' and 'cld-eurocs' refer to results from LES of relative humidity and cloud cover respectively.
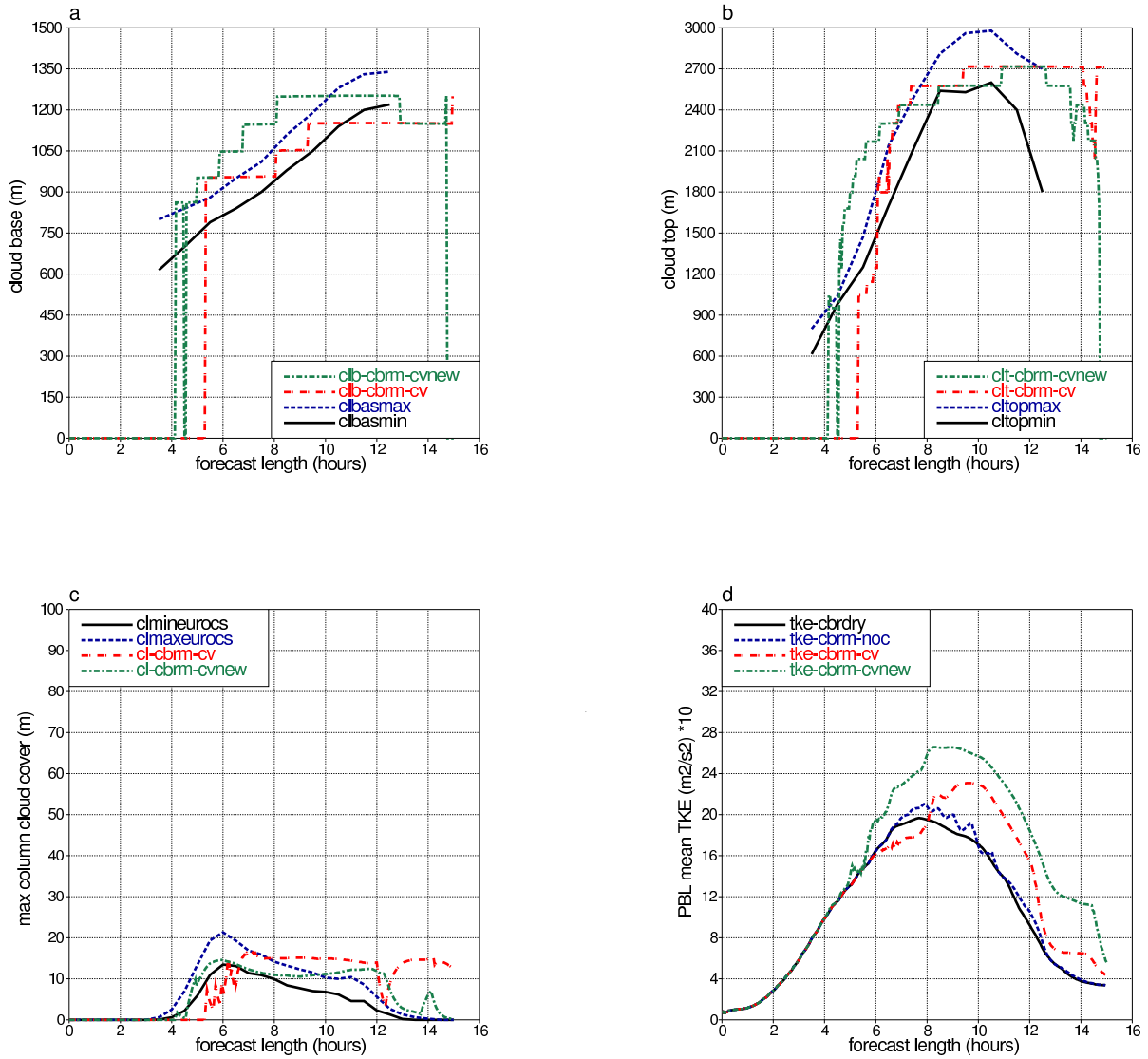
Figure 7: Time dependent results of cloud base height (a), cloud top height (b) , maximum cloud cover among model levels (c), turbulent mean kinetic energy below 900 hPa (d). 'clbasmin', 'clbasmax' refer to minimum and maximum respectively of LES computed cloud base height. 'cltopmin', 'cltopmax' respectively refer to minimum and maximum of cloud top height from LES. 'clmineurocs', 'clmaxeurocs' refer, respectively, to minimum and maximum determination of layer max cloud cover from LES.

8 Acknowledgments

References

Albrecht, B. A., Bretherton, C., Johnson, D., Scubert, W. H., and Frisch, A. S. (1995). The atlantic stratocumulus transition experiment. *Bul. Amer. Meteorol. Soc.*, 76:889–904.

Bougeault, P. (1984). The diurnal cycle of the marine stratocumulus layer: A higher order model study. *J. Atmos. Sci.*, 42:2826–2843.

Bougeault, P. and Lacarrere, P. (1989). Parameterization of orography-induced turbulence in a meso-beta scale model. *Mon. Wea. Rev.*, 117:1872–1890.

Braham, R. (1952). The water and energy budgets of the thunderstorm and their relation to thunderstorm development. *J. Meteor.*, 9:227–242.

Bretherton, C., Austin, P., and Siems, S. (1995). Cloudiness and marine boundary layer dynamics in the astex lagrangian experiments. part ii: Cloudiness, drizzle, surface fluxes, and entrainment. *J. Atmos. Sci.*, 52:2724–2735.

Bretherton, C. and Pincus, R. (1995). Cloudiness and marine boundary layer dynamics in the astex lagrangian experiments. part1: Synoptic setting and vertical structure. *J. Atmos. Sci.*, 52:2707–2723.

Brown, A., Cederwall, R., Chlond, A., Duynkerke, P., Golaz, J.-C., Khairoutdinov, M., Lewellen, D., Lock, A., Macvean, M., Moeng, C.-H., Neggers, R., Siebesma, A., and Stevens, B. (2002). Large-eddy simulation of the diurnal cycle of shallow cumulus convection over land. *Q.J.R. Meteorol. Soc.*, 128:1075–1093.

Chen, C. and Cotton, W. R. (1987). The physics of the marine stratocumulus-capped mixed layer. *J. Atmos. Sci.*, 44:2951–2977.

Cotton, W. R. and Triopli, G. J. (1978). Cumulus convection in shear flow - three-dimensional numerical experiments. *J. Atmos. Sci.*, 35:1503–1521.

Cuxart, J., Bougeault, P., and Redelsperger, J.-L. (2000). A turbulence scheme allowing for meso-scale and large-eddy simulations. *Quart. J. Roy. Meteorol. Soc.*, 126:1–30.

Deardorff, J. (1980). Cloud top entrainment instability. *J. Atmos. Sci.*, 37:131–147.

Duynkerke, P. and Driedonks, A. (1988). The turbulent structure of a shear-driven stratus topped atmospheric boundary layer. *J. Atmos. Sci.*, 45:2343–2351.

Duynkerke, P., Zhang, H., and Jonker, P. J. (1995). Microphysical and turbulent structure of nocturnal stratocumulus as observed during astex. *J. Atmos. Sci.*, 52:2763–2777.

Holtslag, B., Lenderink, G., Siebesma, P., and Sass, B. H. (1998). Turbulence parameterizations for HIRLAM. *LAM Newsletter*, 31:7–11.

Lenderink, G. (2002). Recent and future developments in turbulence modeling in hirlam. *HIRLAM Newsletter*, 41:55–60.

Lenderink, G., Siebesma, A., Cheinet, S., Irons, S., Jones, C., Marquet, P., Müller, F., Olmeda, D., calvo, J., Sánchez, E., and Soares, P. (2004). The diurnal cycle of sjhallow cumulus clouds over land: A single-column model intercomparison study. *Q.J.R. Meteorol. Soc.*, 130:3339–3364.

Malkus, J. and Scorer, R. (1955). The erosion of cumulus towers. *J. Meteorology*, 12:43–57.

McCarthy, J. (1974). Field verification of the relationship between entrainment rate and cumulus cloud diameter. *J. Atmos. Sci.*, 31:1028–1039.

Nitta, T. and Esbensen, S. (1974). Heat and moisture budget analysis using bomex data. *Mon. Wea. Rev.*, 102:17–28.

Paluch, I. (1979). The entrainment mechanism in colorado cumuli. *J. Atmos. Sci.*, 36:2462–2478.

Pruppacher, H. and Klett, J. (1978). *Microphysics of clouds and precipitation*. Kluwer Academic Publishers.

Randall, D. (1984). Stratocumulus deepening through entrainment. *Tellus*, 36A:446–457.

Sass, B. (2001). Modelling of the time evolution of low tropospheric clouds capped by a stable layer. *HIRLAM Tech. Report*, 50:1–43.

Sass, B. H. (2007). A documentation of the STRACO cloud scheme. DMI technical report, Danish Meteorological Institute (in preparation).

Scorer, R. (1957). Experiments on convection of isolated masses of buoyant fluid. *J. Fluid Mech.*, 2:583–594.

Siebesma, A. and Cuipers, J. (1995). Evaluation of parametric assumptions for shallow cumulus convection. *J. Atmos. Sci.*, 52:650–666.

Undén, P., Rontu, L., Calvo, J., Cats, G., Cuxart, J., Eerola, K., Fortelius, C., Garcia-Moya, J. A., Gustafsson, N., Jones, C., Järvenoja, S., Järvinen, H., Lynch, P., McDonald, A., MsGrath, R., Nvascues, B., Odegaard, V., Rodriguez, E., Rummukainen, M., Rõõm, R., Sattler, K., Savijärvi, H., Sass, B. H., Schreur, B. W., The, H., and Tijm, S. (2002). The HIRLAM-5 scientific documentation. HIRLAM-5 project, SMHI Norrköping, Sweden.

Weaver, C. and Pearson, R. (1990). Entrainment instability and vertical motion as courses of stratocumulus breakup. *Q. J. R. Meteorol. Soc.*, 116:1359–1388.